# Interfacial Tension Theory of Low and High Molecular Weight Liquid Mixtures

**Claudia I. Poser† and Isaac C. Sanchez***

*Polymer Science and Engineering Department and Materials Research Laboratory, University of Massachusetts, Amherst, Massachusetts 01003, and Center for Materials Science, National Bureau of Standards, Washington, D.C. 20234.* *Received July 10, 1980*

ABSTRACT: A generalized van der Waals or density gradient theory of interfaces has been combined with a compressible lattice theory of homogeneous fluid mixtures. Binary liquid–vapor and liquid–liquid systems are treated. For nonpolar low molecular weight mixtures, liquid–vapor tensions are calculated as a function of composition with an error of less than 5%. These calculations involve no adjustable parameters; all required parameters are determined from pure-component properties. For polymer solutions, it is usually necessary to introduce an adjustable interaction parameter to accurately correlate liquid–vapor tensions. Approximate equations for the interfacial tension and thickness between two immiscible, high molecular weight polymer liquids have been obtained. These equations are a function of a single interaction parameter; when this parameter is chosen to match experimental tensions, interfacial thicknesses of 1–5 nm are obtained. To assess the importance of compressibility effects, the interaction parameter can be chosen so that the heat of mixing is zero for an incompressible system. This "pure compressibility approximation" works well for polymer pairs with relatively low interfacial tensions. The most serious deficiency of the theory is that intramolecular correlational effects present in long polymer chains are only crudely approximated.

## I. Introduction

In a previous paper,[1] hereafter referred to as I, a theory treating the liquid–vapor interface of pure liquids and polymer melts was presented. This theory was developed by combining the lattice fluid (LF) model[2-5] with the density gradient theory[6-9] of inhomogeneous systems. For nonpolar and slightly polar molecules, this theory was found to work remarkably well. In the present paper, the treatment is generalized to $n$ components, and the results are compared to experimental data for binary liquid–vapor and liquid–liquid systems.

The interfacial properties of binary systems, particularly polymeric ones, have received considerable attention from theorists[10-19] in recent years. An accurate description of polymer interfaces is important because phase separation and immiscibility are the rule rather than the exception for polymer mixtures. In commercial phase-separated polymer blends the interfacial tension is a crucial factor in the adhesive bonding between phases. In addition, the interfacial tensions of poymer solutions are of interest for such applications as enhanced oil recovery.

Section II contains a simple derivation of the general interfacial tension theory for $n$ components. In section III, the LF model for binary mixtures is summarized, and section IV describes the form of the interfacial tension equations for binary systems. Numerical results for binary liquid–vapor systems are discussed in section V. In section VI an approximate theory of poymeric liquid–liquid interfaces is presented. The reader may benefit by first reading section VII, the Discussion.

## II. General Interfacial Tension Theory

The interfacial tension, $\gamma$, for a planar interface can be defined as

$$\gamma \equiv (A - A_e)/S_0 \tag{1}$$

where $S_0$ is the surface area, $A$ is the inhomogeneous system's Helmholtz free energy, and $A_e$ is the Helmholtz free energy of a hypothetical homogeneous system of the same density and composition. In order to evaluate $A$, we adopt the standard assumption[7,20] that the entropy of the inhomogeneous system is only a function of the local density and independent of density gradients. For polymer molecules, the validity of this assumption is expected to be limited. A detailed analysis of this limitation is presented in the Discussion.

Effects of density gradients on the potential energy, $E$, are evaluated in a mean-field approximation. The potential energy per unit volume, $V$, and position $\mathbf{R}$ for an $n$-component system with pairwise additive interactions can be written as

$$E(\mathbf{R})/V = (1/2)\sum_i^n \sum_j^n \epsilon_{ij}(\mathbf{R}) \tag{2}$$

where $\epsilon_{ij}$ is the interaction energy of components $i$ and $j$ and is given by

$$\epsilon_{ij}(\mathbf{R}) = \rho_i(\mathbf{R}) \int \rho_j(\mathbf{R} + \mathbf{s}) u_{ij}(\mathbf{s})\, d\mathbf{s} \tag{3}$$

$\rho_i$ and $\rho_j$ are the densities of components $i$ and $j$, $s \equiv |\mathbf{s}|$ is the intermolecular distance, and $u_{ij}$ is the intermolecular interaction potential, which is assumed to be spherically symmetric. Now $\rho_j(\mathbf{R} + \mathbf{s})$ is expanded in a Taylor series around $\mathbf{s} = 0$

$$\rho_j(\mathbf{R} + \mathbf{s}) = \rho_j(\mathbf{P}) + (\mathbf{s}\cdot\nabla)\rho_j + (1/2!)(\mathbf{s}\cdot\nabla)^2\rho_j + \ldots \tag{4}$$

Substitution of eq 4 into eq 3 and subsequent integration yields

$$\epsilon_{ij} = -\rho_i(\mathbf{R})\rho_j(\mathbf{R})\kappa_0{}^{ij} + \rho_i(\mathbf{R}) \int \{(\mathbf{s}\cdot\nabla)\rho_j + (1/2)(\mathbf{s}\cdot\nabla)^2\rho_j + \ldots\} u_{ij}(\mathbf{s})\, d\mathbf{s} \tag{5}$$

with

$$\kappa_0{}^{ij} = -4\pi \int_{\sigma_{ij}}^{\infty} s^2 u_{ij}(s)\, ds \tag{6}$$

where $\sigma_{ij}{}^3$ is the repulsive core volume between components $i$ and $j$. Since $u_{ij}$ is spherically symmetric, it is an even function of $s_x$, $s_y$, and $s_z$, so that the integral in eq 5 has the following properties:

$$\begin{aligned} \int (\mathbf{s}\cdot\nabla)^b \rho_j u_{ij}(s)\, d\mathbf{s} &= 0 \qquad b \text{ odd} \\ \int (\mathbf{s}\cdot\nabla)^b \rho_j u_{ij}(s)\, d\mathbf{s} &\neq 0 \qquad b \text{ even} \end{aligned} \tag{7}$$

After integration eq 5 becomes

* To whom correspondence should be addressed at the National Bureau of Standards.
† NBS guest worker. Present address: 3M Co., St. Paul, Minn. 55101.

$$\epsilon_{ij} = -\rho_i(\mathbf{R})\rho_j(\mathbf{R})\kappa_0^{ij} - \rho_i(\mathbf{R})\nabla^2\rho_j(\mathbf{R})\kappa_2^{ij} + \ldots \quad (8)$$

with

$$\kappa_2^{ij} = -2\pi/3\int_{\sigma_{ij}}^{\infty} s^4 u_{ij}(s)\, ds \quad (9)$$

Neglecting fourth- and higher order terms in eq 8 is the usual gradient approximation.[6-9] Defining the local Helmholtz free energy density $a_0(\mathbf{R})$ as

$$a_0(\mathbf{R}) \equiv -(1/2)\sum_i\sum_j \rho_i(\mathbf{R})\rho_j(\mathbf{R})\kappa_0^{ij} - TS(\rho_1,\rho_2,\ldots,\rho_n) \quad (10)$$

where $T$ is the temperature and $S$ is the entropy per unit volume, results in the following expression for the Helmholtz free energy density of an inhomogeneous system:

$$a(\mathbf{R}) = a_0(\mathbf{R}) - (1/2)\sum_i\sum_j \rho_i(\mathbf{R})\nabla^2\rho_j(\mathbf{R})\kappa_2^{ij} \quad (11)$$

The total Helmholtz free energy for a system with a planar interface of area $S_0$ and volume $LS_0$ is

$$A = S_0\int_{-L/2}^{L/2}[a_0(x) + (1/2)\sum_i\sum_j \rho_i(x)\, d^2\rho_j(x)/dx^2\, \kappa_2^{ij}]\, dx \quad (12)$$

Integration by parts of the second term in the integral leads to further simplification ($d\rho_i/dx \to 0$ as $L \to \infty$)

$$A = S_0\int_{-L/2}^{L/2}[a_0(x) + (1/2)\sum_i\sum_j \kappa_2^{ij}(d\rho_i/dx)(d\rho_j/dx)]\, dx \quad (13)$$

The final expression for the interfacial tension is

$$\gamma = \int_{-\infty}^{\infty}[\Delta a + (1/2)\sum_i\sum_j \kappa_2^{ij}(d\rho_i/dx)(d\rho_j/dx)]\, dx \quad (14)$$

where

$$\begin{aligned}\Delta a &\equiv a_0(x) - A_e/V \\ &\equiv a_0(x) - \sum_i \rho_i(s)\mu_i^e + P_e\end{aligned} \quad (15)$$

$\mu_i^e$ is the equilibrium chemical potential and $P_e$ is the external pressure.

Minimization of eq 14 yields $n$-coupled differential equations (Euler–Lagrange equations)

$$\begin{aligned}\partial\Delta a/\partial\rho_i - (1/2)\sum_j \kappa_2^{ij}\, d^2\rho_j/dx^2 = 0 \\ i = 1, 2, \ldots, n\end{aligned} \quad (16)$$

Multiplying the differential equations by $d\rho_i/dx$ and summing over species $i$ yields

$$\frac{d}{dx}\left[\Delta a - (1/2)\sum_i\sum_j \kappa_2^{ij}\left(\frac{d\rho_i}{dx}\right)\left(\frac{d\rho_j}{dx}\right)\right] = 0 \quad (17a)$$

which upon integration yields

$$\Delta a = (1/2)\sum_i\sum_j \kappa_2^{ij}(d\rho_i/dx)(d\rho_j/dx) \quad (17b)$$

The equilibrium tension can thus be expressed as

$$\gamma = \sum_i\sum_j \kappa_2^{ij}\int_{-\infty}^{\infty}(d\rho_i/dx)(d\rho_j/dx)\, dx = 2\int_{-\infty}^{\infty}\Delta a\, dx \quad (18)$$

Equation 18 was first derived by Bongiorno, Scriven, and Davis[9] by a different procedure. For a single component these equations reduce to the well-known Cahn–Hilliard equations[7] which were employed in I. The derivation given above is quite general, and the resulting expression for the interfacial tension can be applied to any mean-field fluid model which provides an expression for the equilibrium chemical potential and a specific form of the intermolecular interaction potential.

## III. Lattice Fluid Theory

The generalized version of the LF theory as applied to mixtures has been described in detail elsewhere.[21] The model is evaluated in a mean-field approximation and is formally similar to the Flory–Huggins model of polymer solutions, except that the lattice contains an equilibrium number of vacant sites. This compressible lattice model is thus able to describe density-related phenomena such as lower critical solution temperatures.

In the LF model, three parameters, either $\epsilon^*$, $v^*$, and $r$ or $T^*$, $P^*$, and $\rho^*$ serve to characterize a pure component. These parameters are related by the following definitions:

$$\tilde{T} \equiv T/T^* \qquad T^* \equiv \epsilon^*/k \quad (19)$$

$$\tilde{P} \equiv P/P^* \qquad P^* \equiv \epsilon^*/v^* \quad (20)$$

$$\tilde{V} \equiv 1/\tilde{\rho} \equiv V/V^* \qquad V^* \equiv N(rv^*) \equiv N(M/\rho^*) \quad (21)$$

where $\epsilon^*$ is the total interaction energy per mer, $v^*$ is the close-packed mer volume, $V^*$ is the close-packed volume of the $N$ $r$-mers, $\rho^*$ is the close-packed mass density, and $M$ is the molecular weight. $\tilde{T}$, $\tilde{P}$, $\tilde{v}$, and $\tilde{\rho}$ are the reduced temperature, pressure, volume, and density and $T$, $P$, and $V$ are the temperature, pressure, and volume. The three parameters required to describe a fluid can be readily calculated by using $PVT$ data and have been tabulated for a large number of low molecular weight fluids[2] and a number of common polymers.[4,5]

In the description of a binary mixture, "combining rules" are invoked to describe the interaction energy between unlike mers and the close-packed volume per mer. The combining rules used in this work are given below

$$\epsilon_{12}^* \equiv \zeta(\epsilon_{11}^*\epsilon_{22}^*)^{1/2} \quad (22)$$

$\epsilon_{ij}^*$ is the interaction energy between mers of types 1 and 2, and the close-packed volume per mer of the mixture is

$$v^* \equiv \phi_1 v_1^* + \phi_2 v_2^* - \phi_1\phi_2\delta(v_1^* + v_2^*) \quad (23)$$

$\phi_1$ and $\phi_2$ are the mer fractions of components 1 and 2, and $\zeta$ and $\delta$ are dimensionless parameters which can be evaluated by using an enthalpy and volume of mixing or a critical solution temperature and its critical composition.

The chemical potential for component 1 in a binary mixture is[21]

$$\mu_1 = kT\{\ln\phi_1 + (1 - r_1/r_2)\phi_2\} + r_1\chi_{12}\phi_2^2 \quad (24)$$

where

$$\chi_{12} = \tilde{\rho}X_{12}/kT + (\tilde{P}_1\tilde{v}/\tilde{T}_1)(1 + \nu^{-1})\delta + \phi_2^{-2}\{-\tilde{\rho}/\tilde{T}_1 + \tilde{P}_1\tilde{v}/\tilde{T}_1 + \tilde{v}[(1 - \tilde{\rho})\ln(1 - \tilde{\rho}) + (\tilde{\rho}/r_1)\ln\tilde{\rho}]\} \quad (25)$$

$$X_{12} = (P_1^*P_2^*)^{1/2}v_1^*(v_2^*/v^*)^2\{a + b_{12}\delta + c_{12}\delta^2\} \quad (26)$$

$$a = (\tau/\nu)^{1/2} + (\nu/\tau)^{1/2} - (\nu^{1/2} + \nu^{-1/2})\zeta \quad (27)$$

$$b_{12} = \{\phi_1(2 + \nu\phi_1)(\tau^{1/2} - \zeta) - \phi_2^2(\zeta - \tau^{-1/2})\}(\nu^{1/2} + \nu^{-1/2}) \quad (28)$$

$$c_{12} = \phi_2(\tau^{1/2} - \zeta)(1 + \nu)(\nu^{1/2} + \nu^{-1/2}) \quad (29)$$

$$\begin{aligned}\tau &\equiv \epsilon_{11}^*/\epsilon_{22}^* \equiv T_1^*/T_2^* \\ \nu &\equiv v_1^*/v_2^* = \sigma_{11}^3/\sigma_{22}^3\end{aligned} \quad (30)$$

Exchanging subscripts in eq 24–30 will result in the chemical potential for component 2. Also notice that these equations simplify considerably for $\delta = 0$.

The equation of state of the system can be obtained by minimizing the total free energy with respect to the reduced volume, resulting in

$$\tilde{p}^2 + \tilde{P} + \tilde{T}\{\ln(1-\tilde{p}) + (1-1/r)\tilde{p}\} = 0 \quad (31)$$

This equation is formally identical with the equation of state of a pure system,[2] but $v^*$ is given by eq 23 and the other two characteristic parameters are

$$\epsilon^* \equiv (\phi_1^2 v_1^* \epsilon_{11}^* + \phi_1\phi_2(v_1^* + v_2^*) \times (1+\delta)\zeta(\epsilon_{11}^*\epsilon_{22}^*)^{1/2} + \phi_2^2 v_2^* \epsilon_{22}^*)/v^* \quad (32)$$

$$r \equiv (\phi_1/r_1 + \phi_2/r_2)^{-1} \quad (33)$$

The equation of state defines the value of $\tilde{\rho}$ which will minimize the free energy for given $\tilde{P}$ and $\tilde{T}$.

For two components, given $\epsilon^*$, $v^*$, $r$, and the two mixing parameters $\zeta$ and $\delta$, the LF chemical potential and equation of state can be used to calculate the phase diagram. For a miscible liquid–vapor system, the composition in the vapor phase and the vapor pressure can be calculated at any liquid composition. The compositions of the two liquid phases present in a phase-separated system can also be calculated at a given temperature and pressure. Such calculations are carried out by equating the chemical potentials of each component in the two phases.

## IV. Interfacial Tension Theory for Binary Mixtures

For a binary mixture, the governing equations for the interface may be written

$$\gamma = \int_{-\infty}^{\infty}\{\Delta a + (1/2)[\kappa_{11}\rho_1'^2 + 2\kappa_{12}\rho_1'\rho_2' + \kappa_{22}\rho_2'^2]\}\,dx \quad (34)$$

subject to

$$\frac{\partial \Delta a}{\partial \rho_1} - \kappa_{11}\rho_1'' - \kappa_{12}\rho_2'' = 0 \quad (35a)$$

$$\frac{\partial \Delta a}{\partial \rho_2} - \kappa_{12}\rho_1'' - \kappa_{22}\rho_2'' = 0 \quad (35b)$$

where the following simplified notation has been introduced:

$$\kappa_{ij} \equiv \kappa_2^{ij} \quad (36)$$

$$\rho_i' \equiv d\rho_i/dx \qquad \rho_i'' \equiv d^2\rho_i/dx^2 \quad (37)$$

We will use an inverse power law for the attractive part of the mer–mer interaction potential

$$u_{ij}(s) = \infty \qquad s < \sigma_{ij}$$
$$u_{ij}(s) = -\epsilon_0^{ij}(\sigma_{ij}/s)^m \qquad s \geq \sigma_{ij} \quad (38)$$

In general, the exponent $m$ depends on the $i,j$ interaction so that from eq 9, we obtain

$$\kappa_{ij} = 2\epsilon_{ij}^*\sigma_{ij}^5\tilde{\kappa}_{ij} \quad (39)$$

where

$$\epsilon_{ij}^* \equiv 2\pi\epsilon_0^{ij}/(m_{ij}-3) \quad (40)$$

and

$$\tilde{\kappa}_{ij} \equiv [(m_{ij}-3)/(m_{ij}-5)]/6 \quad (41)$$

Making the identification $\sigma_{ii}^3 \equiv v_i^*$, the cross term $\kappa_{12}$ can be evaluated by using the combining rules

$$\kappa_{12} = 2\zeta(\epsilon_{11}^*\epsilon_{22}^*)^{1/2}[\tfrac{1}{2}(v_1^* + v_2^*)(\delta+1)]^{5/3}\tilde{\kappa}_{12} \quad (42)$$

Alternately, $\kappa_{12}$ can be treated as an adjustable parameter. As shown by Carey,[10,22] a useful simplification in the Euler equations can be achieved when $\kappa_{12}$ is assumed to be given by

$$\kappa_{12} = (\kappa_{11}\kappa_{22})^{1/2} \quad (43)$$

Equation 35 then reduces to the algebraic form

$$\kappa_{22}^{1/2}(\partial\Delta a/\partial\rho_1) - \kappa_{11}^{1/2}(\partial\Delta a/\partial\rho_2) = 0 \quad (44)$$

Both methods of evaluating $\kappa_{12}$ have been employed, with special emphasis on the latter, due to the considerable simplification afforded by eq 44. For convenience in the discussion which follows, we define the dimensionless parameter

$$\omega \equiv \kappa_{12}/(\kappa_{11}\kappa_{22})^{1/2} \quad (45)$$

which expresses the deviation of $\kappa_{12}$ from the geometric mean approximation.

$\omega = 1$ represents the upper limit of permissible values for $\kappa_{12}$. This can be seen by examining eq 17 for a binary mixture

$$\Delta a = (1/2)[\kappa_{11}\rho_1'^2 + 2\kappa_{12}\rho_1'\rho_2' + \kappa_{22}\rho_2'^2] \quad (46)$$

Clearly, if $\gamma$ is to be positive, $\Delta a$ must be positive, so that the quadratic form on the right-hand side of eq 46 must be positive definite. Since the $x$ derivatives of $\rho_1$ and $\rho_2$ can be either positive or negative, $\kappa_{12} < (\kappa_{11}\kappa_{22})^{1/2}$ or equivalently $\omega < 1$ is a necessary condition if the quadratic form is to be positive definite.

Numerical and analytical analysis is facilitated by transforming the equations from $x$ space to $\rho$ space.[10] Such a transformation changes the limits of the integral in eq 34 from infinite to finite. Equation 46 can be rewritten as

$$\rho_1' = \pm\left[\frac{2\Delta a}{\kappa_{11} + 2\kappa_{12}(d\rho_2/d\rho_1) + \kappa_{22}(d\rho_2/d\rho_1)^2}\right]^{1/2} \quad (47)$$

Using this result to effect a change of variables in eq 34 yields

$$\gamma = 2^{1/2}\int_{\rho_1^{\mathrm{I}}}^{\rho_1^{\mathrm{II}}}[\kappa_{11} + 2\kappa_{12}(d\rho_2/d\rho_1) + \kappa_{22}(d\rho_2/d\rho_1)^2]^{1/2}\Delta a^{1/2}\,d\rho_1 \quad (48)$$

where I and II refer to the two equilibrium phases. Equation 47 can also be formally integrated to yield the interfacial tension profile

$$x - x_0 = \int_{\rho_1(x_0)}^{\rho_1(x)}[\kappa_{11} + 2\kappa_{12}(d\rho_2/d\rho_1) + \kappa_{22}(d\rho_2/d\rho_1)^2]^{1/2}\Delta a^{-1/2}\,d\rho_1 \quad (49)$$

When the geometric mean approximation is used for $\kappa_{12}$, eq 44 is the minimization condition for eq 48. If $\kappa_{12}$ is not equal to the geometric mean, eq 35 must be used, which reduces in $\rho$ space to

$$[\kappa_{11} + 2\kappa_{12}(d\rho_2/d\rho_1) + \kappa_{22}(d\rho_2/d\rho_1)^2][(\partial\Delta a/\partial\rho_2) \times [\kappa_{11} + \kappa_{12}(d\rho_2/d\rho_1)] - (\partial\Delta a/\partial\rho_1)[\kappa_{12} + \kappa_{22}(d\rho_2/d\rho_1)]] - (d^2\rho_2/d\rho_1^2)[2\Delta a(\kappa_{11}\kappa_{22} - \kappa_{12})^2] = 0 \quad (50)$$

Although the equations lose their symmetry and look much more complicated in $\rho$ space, a great deal of computational simplicity is gained from this transformation.

Another simplification which applies only in the case where $\kappa_{12}$ is assumed to follow the geometric mean has been employed in some cases. If one defines a variable

$$\Phi \equiv \kappa_{11}\rho_1^{1/2} + \kappa_{22}\rho_2^{1/2} \quad (51)$$

the interfacial tension relationship may be written

$$\gamma = 2^{1/2}\int_{\Phi^{\mathrm{I}}}^{\Phi^{\mathrm{II}}}\Delta a^{1/2}\,d\Phi \quad (52)$$

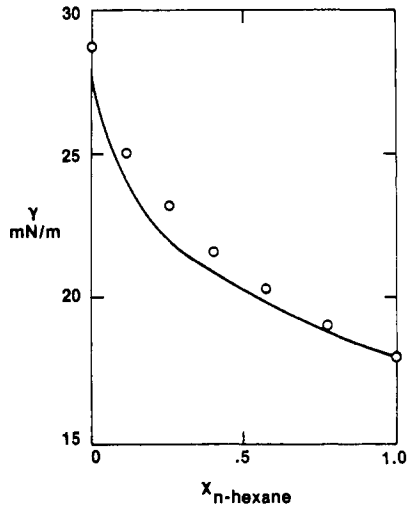


**Figure 1.** Interfacial tension vs. mole fraction for benzene–*n*-hexane at 25 °C. Experimental values were taken from ref 29. The theoretical line was calculated with the following parameters: $\delta = -0.0027$, $\zeta = 0.9688$, $\tilde{\kappa}_{11} = \tilde{\kappa}_{22} = 0.62$, and $\omega = 1$.

and solved subject to eq 44. Care must be exercised in the use of this transformation, since integrating over $\Phi$ from $\Phi^{I}$ (i.e., $\Phi$ evaluated at $\rho_1^{I}$ and $\rho_2^{I}$) to $\Phi^{II}$ implies that $\Phi$ is monotonic. While this is usually true for well-behaved low molecular weight mixtures, there is no guarantee that a smooth profile will result when this assumption is used. The profiles must thus always be monitored simultaneously as a check on such a calculation. A detailed discussion of the numerical techniques employed to solve the interfacial problem for a binary mixture in the various approximations can be found elsewhere.[23]

For the LF theory, the number density of mers, $\rho_i$, is identified as

$$\rho_i \equiv \phi_i \tilde{\rho}/v^* \tag{53}$$

Using this definition along with eq 15, we obtain for the general combining rules

$$\Delta a = \epsilon^* \tilde{\rho}/v^* \{-\tilde{\rho} + \tilde{T}[(\tilde{v} - 1)\ln(1 - \tilde{\rho}) + (1/r)\ln\tilde{\rho} + (\phi_1/r_1)\ln\phi_1 + (\phi_2/r_2)\ln\phi_2]\} + P_e - \tilde{\rho}/v^*(\phi_1\mu_1^e + \phi_2\mu_2^e) \tag{54}$$

The $\mu_i^e$ must be given in units of energy/mer. Equations 34 and 35 can thus be solved by several methods of varying complexity. For liquid–vapor systems, results obtained with $\omega = 1$ were found to differ little from those calculated with $\omega < 1$. For liquid–liquid systems, on the other hand, the results are very sensitive to the value of $\omega$.

## V. Liquid–Vapor Interfaces

**A. Low Molecular Weight Solutions.** In I a constant value of $\tilde{\kappa} = 0.62$ was found to reproduce the interfacial tensions of a wide range of nonpolar and slightly polar low molecular weight liquids over a large temperature interval with an error of about 5%. As an initial assessment of the theory for binary liquid–vapor interfaces, calculations were performed by using the geometric mean approximation for $\kappa_{12}$ ($\omega = 1$) and setting the $\tilde{\kappa}_{ii}$ equal to 0.62. The bulk mixing parameters were set to the values given in Table I, which were obtained from volume and heat-of-mixing data.[24-28] Figure 1 compares the result of such a calculation to experimental data[29] for the benzene–*n*-hexane system. The maximum error in the predicted tension for this mixture is about 5%. Results for the other three systems listed in Table I show similar or slightly greater accuracy.

A part of the error observed for these mixtures is caused by setting $\tilde{\kappa}_{ii} = 0.62$. In order to separate out the error resulting from the mixture theory, we repeated the calculations with pure-component $\tilde{\kappa}$'s which yield the correct pure-component surface tensions. Figure 2 illustrates the type of agreement obtained for benzene–cyclohexane under these conditions. The values of $\tilde{\kappa}$ required were $\tilde{\kappa}_{benzene} = 0.64$ and $\tilde{\kappa}_{cyclohexane} = 0.67$. The maximum error is reduced to 2% for this system. The decrease in the maximum error for benzene–*n*-hexane ($\tilde{\kappa}_{benzene} = 0.64$, $\tilde{\kappa}_{hexane} = 0.62$) was from 5% to 4.2% and for cyclohexane–*n*-benzene ($\tilde{\kappa}_{cyclohexane} = 0.67$, $\tilde{\kappa}_{n\text{-hexane}} = 0.65$) from 4% to 2%. For the benzene–*n*-dodecane system ($\tilde{\kappa}_{benzene} = 0.64$, $\tilde{\kappa}_{n\text{-dodecane}} = 0.59$) the error remained about 1.5%.

Fitting the pure-component $\tilde{\kappa}$'s introduces two additional adjustable parameters into a calculation which is otherwise capable of yielding predictions within 5% without parameter adjustment. For nonpolar mixtures setting the $\tilde{\kappa}$'s equal to 0.62 is quite adequate.

Unfortunately, the four mixtures discussed are the only ones for which both mixing data and reliable interfacial tension data could be located. We therefore investigated the effect of setting $\zeta$ equal to its geometric mean value of 1 and $\delta$ either equal to the arithmetic mean value of 0 or the value appropriate to the geometric mean. [If $\sigma_{12}$ =

**Table I**
**Mixing Parameters for Miscible Liquids**

| | $\delta$ | $\zeta$ | ref |
|---|---|---|---|
| benzene/*n*-hexane | −0.0027 | 0.9688 | 24, 25 |
| cyclohexane/*n*-hexane | −0.0041 | 0.9917 | 26, 27 |
| benzene/cyclohexane | 0.0004 | 0.9635 | 27, 28 |
| benzene/*n*-dodecane | −0.0070 | 0.9521 | 24, 25 |

**Table II**
**Interfacial Tension of Benzene–Cyclohexane at 20 °C for Different Values of the Parameters[a]**

| | | $\gamma_{calcd}$, mN/m | | |
|---|---|---|---|---|
| mole fraction benzene | $\gamma_{expt}$,[b] mN/m | $\zeta = 0.9635$ $\delta = 0.0004$ | $\zeta = 1.0$ $\delta = 0.0$ | $\zeta = 1.0$ $\delta = 0.0001$ (geom mean) |
| 0.1282 | 25.00 | 24.87 | 25.21 | 25.22 |
| 0.2174 | 25.14 | 24.96 | 25.49 | 25.50 |
| 0.4874 | 25.84 | 25.45 | 26.44 | 26.46 |
| 0.6470 | 26.54 | 25.96 | 27.08 | 27.11 |
| 0.7814 | 27.20 | 26.64 | 27.70 | 27.72 |
| 0.9033 | 27.88 | 27.64 | 28.33 | 28.34 |

[a] $\tilde{\kappa}_{benzene} = 0.64$, $\tilde{\kappa}_{cyclohexane} = 0.67$, and $\omega = 1$. [b] Data taken from ref 26.

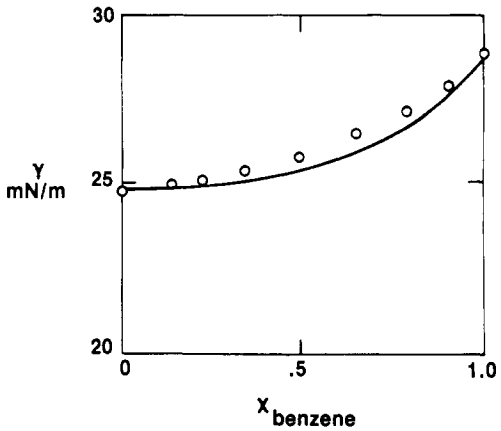


**Figure 2.** Interfacial tension vs. mole fraction for benzene–cyclohexane at 20 °C with fitted end points. Experimental data were taken from ref 29. The theoretical line was calculated with the following parameters: $\delta = -0.0004$, $\zeta = 0.9635$, $\tilde{\kappa}_{benzene} = 0.64$, $\tilde{\kappa}_{cyclohexane} = 0.67$, and $\omega = 1$.

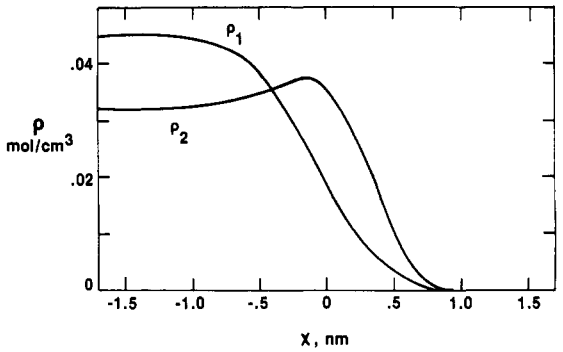


**Figure 3.** Interfacial profiles for benzene–*n*-hexane at 25 °C. Component 1 is benzene. The theoretical line was calculated with a benzene mole fraction of 0.6 and the following parameters: $\delta$ = −0.9927, $\zeta$ = 0.9688, $\tilde{\kappa}_{11} = \tilde{\kappa}_{22}$ = 0.64, and $\omega$ = 1.

$(\sigma_{11}\sigma_{22})^{1/2}$, then $\delta = [2(v_1^* v_1^*)^{1/2} - v_1^* - v_2^*]/(v_1^* + v_2^*)$.] The results of such calculations for benzene and cyclohexane are shown in Table II. The same trends are observed for the other three systems. For these nonpolar systems, the use of $\omega$ = 1, $\delta$ = 0.0, and $\zeta$ = 1.0 results in reasonable predictions, although somewhat less accurate than those obtained with fitted values of $\delta$ and $\zeta$. Since the numerical solution of the interfacial equations with $\omega$ < 1 requires about twice the computational time of the solution with $\omega$ = 1, the latter was used for all further liquid–vapor calculations.

In the further examination of the present mixture theory's predictions, the concept of an "ideal" interfacial tension, $\gamma_{id}$, is useful. This quantity is defined by

$$\gamma_{id} \equiv x_1\gamma_1 + x_2\gamma_2 \tag{55}$$

where $x_i$ are mole fractions. In general, experimentally observed tensions of mixtures fall below $\gamma_{id}$. Such negative deviations are associated with the preferential adsorption of the lower tension component at the interface. Figure 3 shows the calculated interfacial profiles for benzene–*n*-hexane at 25 °C. These profiles clearly demonstrate the ability of the present theory to predict preferential adsorption phenomena.

The system benzene–*n*-dodecane exhibits an extremely negative deviation from $\gamma_{id}$. Schmidt and Clever[30,31] attempted to explain the unusual shape of the experimental benzene–*n*-dodecane curve by postulating a layer of *n*-dodecane molecules oriented perpendicularly to the surface. They advanced a similar picture to account for the positive deviation from $\gamma_{id}$ in *n*-dodecane–*n*-hexane mixtures. The present theory correctly predicts both the shape of the benzene–*n*-dodecane curve and the positive deviation for *n*-dodecane–*n*-hexane, without invoking orientational effects. Positive deviations from $\gamma_{id}$ are particularly puzzling, since energetic arguments cannot provide a basis for such results for nonpolar mixtures. We found, however, that the observed positive deviations for the *n*-dodecane–*n*-hexane mixture can be removed if the size difference between the molecules is taken into account. Recalling the definition of the mer fraction (physically, it is roughly equal to the volume or weight fraction of the component)

$$\phi_i = r_i N_i / rN \tag{56}$$

we define a new ideal surface tension based on mer fractions

$$\gamma_{id}' \equiv \phi_1\gamma_1 + \phi_2\gamma_2 \tag{57}$$

and plot the experimental and theoretical values of $\gamma$ vs. $\phi_1$. Figure 4 shows this plot. The semidashed line represents eq 57. Both the data and the calculated line now exhibit a small negative deviation from the ideal value.

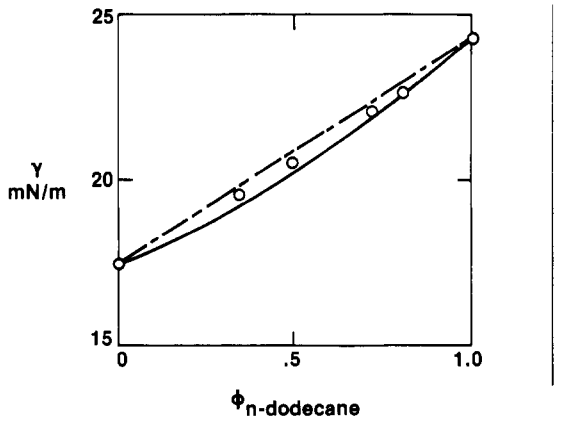


**Figure 4.** Interfacial tension vs. mer fraction for *n*-dodecane–*n*-hexane at 30 °C. Experimental data were taken from ref 30. The theoretical line (solid) was calculated with the following parameters: $\delta$ = 0.0, $\zeta$ = 1.0, $\tilde{\kappa}_{n\text{-dodecane}}$ = 0.59, $\tilde{\kappa}_{n\text{-hexane}}$ = 0.62, and $\omega$ = 1. The semidashed line is the ideal tension given by eq 57.

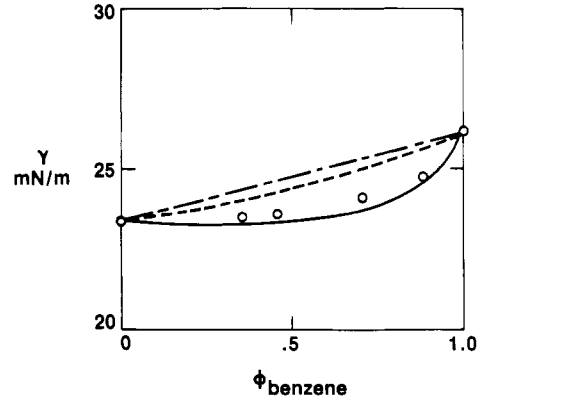


**Figure 5.** Interfacial tension vs. mer fraction for benzene–*n*-dodecane at 40 °C. Experimental data were taken from ref 31. The broken line was calculated with $\delta$ = 0.0 and $\zeta$ = 1.0. The solid line was obtained from $\delta$ = −0.0070 and $\zeta$ = 0.9521. For both calculations, $\tilde{\kappa}_{n\text{-dodecane}}$ = 0.59, $\tilde{\kappa}_{benzene}$ = 0.64, and $\omega$ = 1. The semidashed line is the ideal tension given by eq 57.

The moral here is that molecules in a mixture contribute to the surface tension not according to their number but according to their number and size. This is the essential conclusion of the monolayer theory for polymer solutions as originally formulated by Prigogine and Marechal.[32]

When the benzene–*n*-dodecane data are plotted in terms of mer fractions, the negative deviations from ideal behavior are somewhat less extreme, but still sizable. Figure 5 compares the data to the values calculated with $\delta$ = −0.0070 and $\zeta$ = 0.9521 (solid line) and to those calculated with $\delta$ = 0.0 and $\zeta$ = 1.0 (broken line). Clearly, the theory is only able to predict the data well using the fitted mixture parameters. Thus, the present theory suggests that the unusually large negative deviations in this system are related to the relatively large deviation from ideal mixing behavior. This idea is further supported by qualitative differences in the calculated density profiles. For $\delta$ = 0 and $\zeta$ = 1.0 the density profiles are monotonic, whereas for the fitted parameters, an adsorption peak appears in the *n*-dodecane profile. The less favorable mixing parameters lead to a lower interfacial tension because the adsorption of the *n*-dodecane in the interfacial layer minimizes the number of unfavorable interactions between benzene and dodecane. The present theory is thus able to predict the dependence of the interfacial tension–composition behavior farily accurately for low molecular weight binary mixtures by accounting for size differences and the effect of unfavorable unlike contacts.

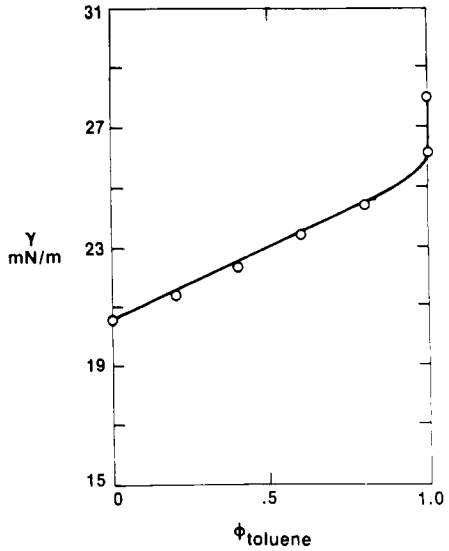


**Figure 6.** Interfacial tension vs. volume fraction for toluene–poly(dimethylsiloxane) at 24 °C. Experimental data were taken from ref 33. The theoretical line was calculated with $\delta = 0.0$, $\zeta = 1.0$, $\bar{\kappa}_{toluene} = 0.62$, $\bar{\kappa}_{PDMS} = 0.49$, and $\omega = 1$.

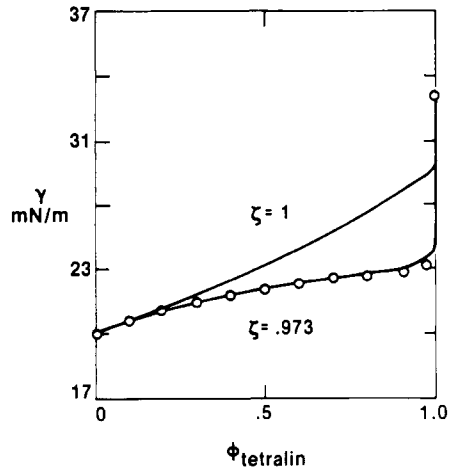


**Figure 7.** Interfacial tension vs. volume fraction for tetralin–poly(dimethylsiloxane) at 30 °C. Experimental data were taken from ref 34. The theoretical lines were calculated with $\delta = 0.0$, $\bar{\kappa}_{tetralin} = 0.77$, $\bar{\kappa}_{PDMS} = 0.49$, and $\omega = 1$.

**B. Polymer Solutions.** An interesting aspect of polymer solution interfacial tension derives from the experimental observation that a polymer added to a solvent of higher tension behaves like a surfactant. In other words, the polymer depresses the interfacial tension drastically at very low polymer concentrations. Figures 6 and 7 compare the experimental data to the theoretical predictions for two systems of this type. $\delta$ was set equal to 0.0 for these calculations. The fit obtained for the toluene–poly(dimethylsiloxane) system with $\zeta = 1.0$ is excellent, whereas for the tetralin–poly(dimethylsiloxane) system, $\zeta = 0.973$ must be used in order to accurately represent the data. Equally good fits have been obtained for the same sets of data by Gaines' monolayer theory.[33] The values used for the monolayer theory's fitting parameter, $\chi$, were 0.106 for toluene–poly(dimethylsiloxane)[33] and 0.85 for tetralin–poly(dimethylsiloxane).[34] In both theories, the interaction parameter used is thus indicative of a less favorable energetic interaction for the tetralin solution.

Figure 8 shows the calculated interfacial profiles for tetralin–poly(dimethylsiloxane) at 0.8 volume fraction of tetralin. For this system, we again observed an increasing adsorption peak with decreasing values of $\zeta$ as in the benzene–*n*-dodecane case. In contrast to *n*-dodecane, the poly(dimethylsiloxane) profile exhibited an adsorption peak even at $\zeta = 1.0$. We also observed that the maximum in the polymer adsorption peak decreased only slightly as a function of increasing tetralin volume fraction, which is consistent with the almost flat tension curve.

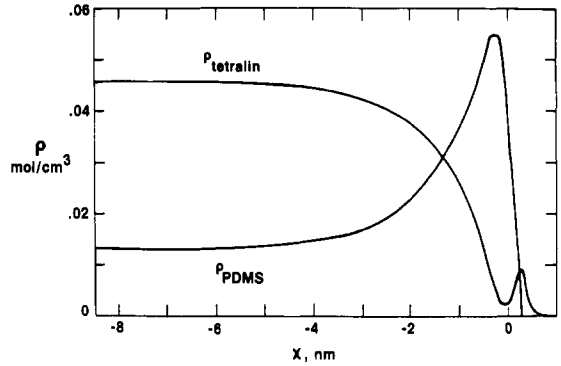


**Figure 8.** Interfacial profiles for tetralin–poly(dimethylsiloxane) at 30 °C. The volume fraction of tetralin was 0.8. Other parameters were $\delta = 0.0$, $\zeta = 0.973$, $\bar{\kappa}_{tetralin} = 0.77$, $\bar{\kappa}_{PDMS} = 0.49$, and $\omega = 1$.

The predictions of the present theory for polymer solutions are comparable in accuracy to Gaines' monolayer approach. However, the conceptually unsatisfying requirement of a single surface layer containing polymers whose conformations are confined to this layer is avoided. In addition, explicit predictions of the interfacial structure can be made.

## VI. Liquid–Liquid Interfaces

Extension of the theory to liquid–liquid interfaces is difficult for two reasons: First, most low molecular weight mixtures that phase separate contain at least one highly polar component.[35] As discussed in I, the theory breaks down for polar liquids. A second reason is that LF theory is a mean-field theory which incorrectly describes the shape of the coexistence curve near the critical temperature. Thus, when LF theory is used in conjunction with the gradient theory, it yields a classical mean-field exponent of 1.5 for the dependence of the interfacial tension on $T_c - T$.[22] The correct exponent is between 1.2 and 1.3.[36]

For the above-mentioned reasons, we only expect the theory to work well for nonpolar or slightly polar liquids far away from a critical point. The best examples of such systems are polymer/polymer liquid mixtures. With these systems, however, other difficulties arise. The calculated phase diagrams are extremely sensitive to the values of the interaction parameters ($\zeta$ and $\delta$). Also, we assumed from the outset that the entropy in the interfacial region is independent of concentration gradients. This is a serious approximation for polymeric systems. Thus, in its present form, the theory is being pushed to its limits when it is applied to a polymer/polymer interface.

To examine the theory for polymer/polymer interfaces we set $\delta$ equal to the appropriate mean value and $\omega = \zeta$. Figure 9 illustrates the molecular weight dependence of the tension and interfacial thickness predicted by theory. The curves were calculated for polyethylene/polystyrene with $\zeta = \omega = 0.98$ and $r_1 = r_2 = r$. The thickness $t$ was defined as

$$t \equiv (dx/d\tilde{\rho}_1)_{\tilde{\rho}_1=1/2} \tag{58}$$

where $\tilde{\rho}_1$ is the mer density of component 1 reduced by the equilibrium value of $\rho_1$ in the phase in which component 1 dominates. As $r$ decreases, mixing becomes more favorable until at some critical value of $r$ (in this case ~100)

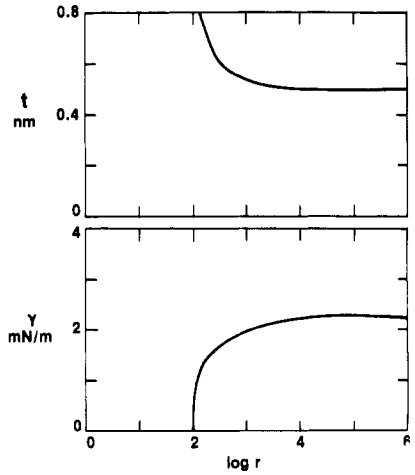


**Figure 9.** Interfacial tension and thickness as a function of molecular weight for linear polyethylene–polystyrene at 140 °C. The curves were calculated with $\delta = -0.0110$, $\omega = 0.98$, $\tilde{\kappa}_{1\text{-PE}} = 0.52$, $\tilde{\kappa}_{PS} = 0.57$ at 50/50 composition.

the system becomes completely miscible. Consequently, the thickness must go to infinity and the tension must go to zero with decreasing $r$. The rapid change in both quantities as $r$ exceeds the critical value followed by an asymptotic dependence at large $r$ is qualitatively in agreement with Roe's lattice theory.[16] If the value of $\zeta$ is decreased, the critical $r$ decreases, and the asymptotic values of the thickness and tension decrease and increase, respectively.

As Figure 9 suggests, the interfacial tension between two polymers approaches an asymptotic limit as the molecular weight of the two polymers becomes very large. Also for two immiscible polymers, the solubility of polymer A in polymer B is proportional to $M_A^{-1}$, where $M_A$ is the molecular weight of polymer A. Similarly, the solubility of B in A is proportional to $M_B^{-1}$. Therefore, as $M_A$ and $M_B$ become very large, the two phases approach pure A and pure B.

We can take advantage of these results to obtain an approximate analytic formula for the interfacial tension and thickness of two infinite molecular weight polymers. To this end, the first approximation that we shall make is to assume that the density through the interface varies linearly with composition; i.e.

$$d\rho/d\rho_1 = \text{constant} = 1 + d\rho_2/d\rho_1 \tag{59a}$$

The constant in eq 59a can be determined by integrating and results in

$$d\rho/d\rho_1 = (\rho_1^0 - \rho_2^0)/\rho_1^0 \tag{59b}$$

$$d\rho_2/d\rho_1 = -\rho_2^0/\rho_1^0 \tag{59c}$$

where $\rho_1^0$ and $\rho_2^0$ are the mer densities of the pure components 1 and 2

$$\rho_i^0 \equiv \tilde{\rho}_i/v_i^* \tag{60}$$

Equation 59 replaces eq 35.

Substituting eq 59 into 48, we obtain

$$\gamma = 2^{1/2}[(\kappa_{11}^{1/2}\rho_1^0)^2 - 2\kappa_{12}\rho_1^0\rho_2^0 + (\kappa_{22}^{1/2}\rho_2^0)^2]^{1/2}\int_0^1 \Delta a^{1/2}\, d\tilde{\rho}_1 \tag{61a}$$

For simplicity in what follows we assume that $\tilde{\kappa}_{ii} = {}^1/_2$ (the value appropriate for an $R^{-6}$ attractive potential) and $\delta = 0$ so that with the help of eq 39, eq 61a becomes

$$\gamma = (2\tilde{\kappa}_0)^{1/2}(\gamma_1^*\gamma_2^*)^{1/4}(v_1^*v_2^*)^{1/12}\int_0^1 \Delta a^{1/2}\, d\tilde{\rho}_1 \tag{61b}$$

where $\tilde{\kappa}_0$ is the dimensionless quantity

$$\tilde{\kappa}_0 \equiv \tau^{1/2}\nu^{-1/6}\tilde{\rho}_1^2 - 2\omega\tilde{\rho}_1\tilde{\rho}_2 + \tau^{-1/2}\nu^{1/6}\tilde{\rho}_2^2 \tag{62}$$

$\omega$ is defined by eq 45 and the $\gamma_i^*$ are the characteristic surface tensions of the pure components

$$\gamma_i^* \equiv \epsilon_{ii}^*/(v_i^*)^{2/3} \equiv P_i^*\sigma_{ii} \tag{63}$$

From eq 54, $\Delta a$ is given by

$$\Delta a = \tilde{\rho}/v^*[a(\tilde{\rho},\tilde{T})\epsilon^* - \phi_1 a(\tilde{\rho}_1,\tilde{T}_1)\epsilon_{11}^* - \phi_2 a(\tilde{\rho}_2,\tilde{T}_2)\epsilon_{22}^*] \tag{64}$$

where

$$a(\tilde{\rho},\tilde{T}) \equiv -\tilde{\rho} + \tilde{T}(1-\tilde{\rho})\ln(1-\tilde{\rho})/\tilde{\rho} \tag{65}$$

The values of $\tilde{\rho}_1$ and $\tilde{\rho}_2$ are determined from the equation of state, eq 31, at their respective reduced temperatures $\tilde{T}_1$ and $\tilde{T}_2$ with $r \to \infty$ and $\tilde{P} = 0$.

$\Delta a$ will reach its maximum value near $\rho = (\rho_1^0 + \rho_2^0)/2$. Therefore, the integral in eq 61 can be approximated by $(\Delta a_{1/2})^{1/2}/2$, where

$$\Delta a_{1/2} \equiv \Delta a_{\rho=(\rho_1^0+\rho_2^0)/2} \tag{66a}$$

Since $\rho = \rho_1 + \rho_2 = \tilde{\rho}/v^*$ and $\phi_1 = \rho_1/\rho$, eq 66a becomes ($\delta = 0$)

$$\Delta a_{1/2} = \tilde{\rho}_{1/2}\{a(\tilde{\rho}_{1/2},\tilde{T}_{1/2})P^* - [a(\tilde{\rho}_1,\tilde{T}_1)\theta_1 P_1^* + a(\tilde{\rho}_2,\tilde{T}_2)\theta_2 P_2^*]\} \tag{66b}$$

where

$$\tilde{\rho}_{1/2} \equiv (\tilde{\rho}_1 + \tilde{\rho}_2)/2 \tag{67}$$

$$\theta_1 \equiv 1 - \theta_2 \equiv \tilde{\rho}_1/(\tilde{\rho}_1 + \tilde{\rho}_2) \tag{68}$$

$$P^* \equiv \theta_1^2 P_1^* + \theta_2^2 P_2^* + \zeta(\nu^{1/2} + \nu^{-1/2})\theta_1\theta_2(P_1^*P_2^*)^{1/2} \tag{69}$$

$$\tilde{T}_{1/2} \equiv \left[\frac{\tilde{\rho}_1\nu^{-1/2} + \tilde{\rho}_2\nu^{1/2}}{\tilde{\rho}_1 + \tilde{\rho}_2}\right]\frac{(P_1^*P_2^*)^{1/2}}{P^*}(\tilde{T}_1\tilde{T}_2)^{1/2} \tag{70}$$

Finally, our approximate equation for the interfacial tension of two polymers of very high molecular weight becomes

$$\gamma = {}^1/_2(2\tilde{\kappa}_0\Delta\tilde{a}_{1/2}\gamma_1^*\gamma_2^*)^{1/2} \tag{71}$$

where $\Delta\tilde{a}_{1/2}$ is a dimensionless free energy defined by

$$\Delta\tilde{a}_{1/2} \equiv \Delta a_{1/2}/(P_1^*P_2^*)^{1/2} \tag{72}$$

From eq 47 and 58, the thickness of the interfacial region is given by

$$t = (\tilde{\kappa}_0/2\Delta\tilde{a}_{1/2})(v_1^*v_2^*)^{1/6} \tag{73}$$

Polymer/polymer interfacial tensions and thicknesses can now be easily calculated from eq 71 and 73 once values of $\zeta$ and $\omega$ are provided. We will assume that $\omega = 0$ and justify this choice in the Discussion.

In Table III we present the values of the interaction parameter $\zeta$ required to reproduce the experimentally observed interfacial tensions for several polymer/polymer mixtures. Table IV contains the pure polymer parameters used in the calculations. The calculated thicknesses from eq 73 are also shown. Notice that most thicknesses are between 1 and 5 nm, which are comparable with those calculated from the theory of Helfand and Sapse.[14] The calculated tensions are very sensitive to the chosen value

Table III
Calculated Interaction Parameters and Interfacial Thickness

| polymer pair | $\gamma_{expt}$,[a] mN/m | $\zeta$ | $\Delta\tilde{a}_{1/2} \times 10^3$ | $\tilde{\kappa}_0$ | $t_{calcd}$, nm |
|---|---|---|---|---|---|
| PS/PMMA | 1.7 | 0.9947 | 0.24 | 1.62 | 5.7 |
| PnBMA/PMMA | 1.9 | 1.0028 | 0.31 | 1.55 | 5.0 |
| PhBMA/PVAc | 2.9 | 0.9952 | 0.78 | 1.46 | 3.2 |
| PS/PVAc | 3.7 | 0.9756 | 1.27 | 1.54 | 2.5 |
| PnBMA/PDMS | 3.8 | 1.0180 | 2.1 | 1.36 | 1.9 |
| PIB/PDMS | 4.2 | 1.0025 | 2.95 | 1.37 | 1.6 |
| b-PE/PDMS | 5.1 | 1.0010 | 4.2 | 1.40 | 1.4 |
| l-PE/PnBMA | 5.3 | 0.9928 | 2.65 | 1.51 | 1.7 |
| l-PE/PS | 5.9 | 0.9854 | 3.4 | 1.59 | 1.5 |
| PS/PDMS | 6.1 | 0.9985 | 5.6 | 1.46 | 1.2 |
| PVAc/PDMS | 7.4 | 1.0050 | 7.65 | 1.33 | 1.0 |
| PIB/PVAc | 7.5 | 0.9770 | 5.65 | 1.47 | 1.2 |
| l-PE/PMMA | 9.7 | 0.9835 | 7.52 | 1.57 | 1.0 |
| l-PE/PVAc | 11.3 | 0.965 | 11.3 | 1.48 | 0.8 |

[a] Data at 140 °C from ref 17.

Table IV
Equation-of-State Parameters[a]

| | $T^*$, K | $P^*$, mN/m$^2$ | $v^*$, cm$^3$/mol | $\gamma^*$, mN/m | $\tilde{\rho}$ at 140 °C |
|---|---|---|---|---|---|
| poly(dimethylsiloxane) | 476 | 302 | 13.1 | 84 | 0.759 |
| poly(vinyl acetate) | 590 | 509 | 9.6 | 128 | 0.845 |
| polyisobutylene | 643 | 354 | 15.1 | 104 | 0.872 |
| polyethylene (linear) | 649 | 425 | 12.7 | 118 | 0.875 |
| polyethylene (branched) | 673 | 359 | 15.6 | 106 | 0.885 |
| polystyrene (atatic) | 735 | 357 | 17.1 | 109 | 0.906 |
| poly(methyl methacrylate) | 693 | 503 | 11.5 | 134 | 0.894 |
| poly(*n*-butyl methacrylate) | 627 | 431 | 12.1 | 117 | 0.864 |

[a] Reference 5.

of the interaction parameter $\zeta$. So although most $\zeta$ values are about 0.99, there is no universal value of $\zeta$ that can be used for all pairs.

For an incompressible lattice, $\tilde{\rho}_1 = \tilde{\rho}_2 = \tilde{\rho}_{1/2} = 1$, $a(\tilde{\rho}_1 = 1, \tilde{T}) = -1$, and, by eq 66b, $\Delta a_{1/2} \sim \Delta P^*$, where $\Delta P^*$ is given by

$$\Delta P^* = P_1^* + P_2^* - \zeta(\nu^{1/2} + \nu^{-1/2})(P_1^* P_2^*)^{1/2} \quad (74)$$

Now $\Delta P^* = 0$ if $\zeta = \zeta_0$, where

$$\zeta_0 = \frac{(\tau/\nu)^{1/2} + (\tau/\nu)^{-1/2}}{\nu^{1/2} + \nu^{-1/2}} \quad (75)$$

For this value of $\zeta$, the heat of mixing is zero for an incompressible system. To assess the importance of compressibility effects we have calculated tensions for $\zeta = \zeta_0$, which are shown in Table V. Calculated tensions are compared to experiment and to those of Helfand and Sapse.[14] None of the polymer pairs involving linear polyethylene are included in Table V because the calculated tensions were uniformly too low. In general, this "pure compressibility approximation" appears to work well only for polymer pairs with low interfacial tensions (less than 6 mN/m) or, equivalently, for pairs where unfavorable energetics can be ignored.

## VII. Discussion

A generalized van der Waals or density gradient theory of interfaces has been combined with a compressible lattice theory of homogenous fluid mixtures. This combined theory has been examined in some detail for binary systems. For binary mixtures there are three gradient coefficients: $\kappa_{11}$, $\kappa_{22}$, and $\kappa_{12}$. The pure-component coefficients $\kappa_{11}$ and $\kappa_{22}$ are determined from pure-component data.

For liquid–vapor interfaces, good predictions of interfacial tensions are obtained for low molecular weight solutions and polymer solutions with the cross coefficient set equal to the geometric mean: $\kappa_{12} = (\kappa_{11}\kappa_{22})^{1/2}$ or $\omega = 1$. For nonpolar low molecular weight mixtures, liquid–vapor tensions are calculated to within 5% for the systems investigated. These results are similar to those previously obtained by Carey et al.[10,22] by combining the gradient theory with the Peng–Robinson equation of state. For similar sized hydrocarbons, these authors found agreement to within 2%. However, this theory cannot be extended to polymer systems.

In some cases, calculated density profiles indicate preferential adsorption of the lower tension component. By accounting for molecular size differences and unfavorable energetic interactions between unlike components, the theory can describe "anomalous systems" without involving ordered surface layers.

Calculated tensions of polymer solution liquid–vapor interfaces are comparable to those obtained by the monolayer theory of Gaines.[32] However, the present theory has the advantage of yielding a density profile.

For liquid–liquid interfaces, the theory is less successful. We have only considered polymer/polymer liquid mixtures far away from any critical point. In this case we set $\kappa_{12} = 0$ or $\omega = 0$. Our rationale for setting the cross coefficient equal to zero is related to our original assumption that concentration gradients affect energies but not entropies. If this assumption is removed, then the $\kappa_{ij}$ are related to second moments of their corresponding *direct correlation functions*.[9,37] Thus, the magnitude of $\kappa_{ij}$ is proportional to a correlation distance (squared), whereas in the present

Table V
Comparison of Theoretical and Experimental Surface Tensions

| | | $\gamma_{calcd}$, mN/m | | $t_{calcd}$, nm | | |
|---|---|---|---|---|---|---|
| polymer pair | $\gamma_{expt}$,[17] mN/m | pure compressibility approx | Helfand and Sapse[14] | pure compressibility approx | Helfand and Sapse[14] | $\zeta_0$ |
| PS/PMMA | 1.7 | 1.0 | 0.3 | 10.0 | 16.0 | 0.9951 |
| PnBMA/PMMA | 1.9 | 2.0 | 1.5 | 4.8 | 2.9 | 1.0027 |
| PnBMA/PVAc | 2.9 | 1.2 | 3.0 | 8.0 | 1.6 | 0.9970 |
| PS/PVAc | 3.7 | 4.0 | 1.9 | 2.3 | 3.1 | 0.9751 |
| PnBMA/PDMS | 3.8 | 4.6 | 3.2 | 1.6 | 1.3 | 0.0150 |
| PIB/PDMS | 4.2 | 4.6 | | 1.5 | | 1.0007 |
| b-PE/PDMS | 5.1 | 5.4 | | 1.3 | | 0.9999 |
| PS/PDMS | 6.1 | 6.8 | | 1.1 | | 0.9947 |
| PVAc/PDMS | 7.4 | 3.8 | 7.2 | 2.0 | 0.8 | 1.0224 |

theory it is proportional to the second moment of an intermolecular pair potential (see eq 9 and 39).

Within the context of the compressible lattice model that we used, the correlation distance is between chain segments or "mers". The intrinsic connectivity of a polymer chain introduces strong mer–mer correlations. For example, in an ideal Gaussian chain, the *intramolecular* mer–mer correlations fall off as $R^{-1}$ ($R \equiv$ distance); in a chain with excluded volume the correlations fall off as $R^{-4/3}$ as shown by Edwards.[38] In the undiluted bulk phase liquid, the intramolecular mer–mer correlations are very short ranged because *intermolecular* mer–mer interactions "screen" the intramolecular excluded-volume effects.[39,40] The "blob model" of Daoud[41,42] is a very convenient method of conceptualizing these correlations.

The salient point is that correlations among mers belonging to the same chain (self-correlation) can be very long ranged, whereas correlations among mers belonging to different chains, in which the connectivity constraint is absent, will always be shorter in range. Since the relative density of a polymer varies from 1 to 0 through a polymer/polymer interface and because self-correlations become strong in the dilute limit, the *average* values of $\kappa_{11}$ and $\kappa_{22}$ should be much larger than the cross term $\kappa_{12}$. We say average values because in the rigorous theory,[9,37] the gradient coefficients are not constants but vary with concentration in the interface. Setting $\kappa_{12} = 0$ or $\omega = 0$ is our crude attempt to take into account these intramolecular correlational effects. We note parenthetically that the Helfand and Sapse theory,[14] in its simplest form, is formally a $\kappa_{12} = 0$ type theory.

Equations 71 and 73 are approximate equations for the interfacial tension and thickness between two high molecular weight polymers. In Table V calculated tensions are compared with available experimental values and with those calculated from the Helfand and Sapse theory.[14] Also included in Table V are interfacial thicknesses as calculated from both theories. The latter are usually in the range of 1–5 nm for both theories. Our calculations assumed $\omega = 0$ and $\zeta = \zeta_0$, where $\zeta_0$ is defined by eq 75. This choice of the interaction parameter $\zeta$ is an energetically neutral choice in that the calculated heat of mixing is zero if it is assumed that the liquids are incompressible. Thus, for this choice of $\zeta$, the only contributions to the mixture free energy arise from compressibility effects. This "pure compressibility approximation" appears to work well for polymer pairs that have relatively low interfacial tensions.

Formally, the present theory of polymer/polymer interfaces looks quite similar to that of Helfand and Sapse (HS).[14] Conceptually, however, they are quite different. Gradient effects on the free energy arise from energetic considerations only in the present theory, whereas they arise only from the intrinsic connectivity of a polymer chain in HS theory. In the simplest version of HS theory compressibility effects are ignored, whereas they play an all-important role in the present theory.

Compressibility effects, which are associated with density variations through the interfacial region, completely dominate liquid–vapor tensions.[43–45] This explains why the present theory works extremely well for both low and high molecular weight solutions. For liquid–liquid interfaces, compressibility effects are less important, but we contend that they cannot be ignored. Some evidence for this assertion is found in Table V, where calculated tensions are carried out in the pure compressibility approximation ($\zeta = \zeta_0$). In this approximation, all calculated tensions would equal zero if the polymer liquids were treated as incompressible. However, allowing for density variations through the interface yields small positive tensions which are in good agreement with experimental values of the polymer pairs shown in Table V.

Conceptually, the present theory more closely resembles the theory of Nose.[12] As in the present theory, Nose begins with a mean-field gradient expansion of the free energy. Energetic effects are taken into account similarly, but Nose also approximately accounts for chain connectivity. However, Nose completely neglects compressibility effects.

In our judgment all current theories of polymer/polymer interfaces, including the present one, contain deficiencies. A proper theory should not ignore the compressible nature of polymer liquids (even though it is very small) nor can it ignore the intrinsic connectivity of a polymer chain. The latter affects the free energy not only in the interfacial region but also in diluted bulk phases becauses it produces inhomogenities.

To clarify this latter point it is convenient to discuss inhomogenity in terms of size scales. At size scales much larger than $\zeta$, the polymer solution appears homogeneous and monomer concentration fluctuations are small. For size scales smaller than $\zeta$, the solution appears inhomogeneous and concentration fluctuations are large. It is obvious that $\zeta$ depends on the degree of interpenetration between polymer chains. In a very dilute solution, $\zeta$ will equal the average distance between chain centers; in undiluted polymer, $\zeta$ is of order of the length of a monomer unit. In semidilute solutions where chains on the average strongly overlap with one another, $\zeta$ is less than the average size of a chain but greater than the size of a monomer unit. According to scaling arguments,[40–42] in the good-solvent semidilute range

$$\zeta \sim c^{-3/4} \tag{76}$$

where $c$ is the global monomer concentration. A characteristic of $\zeta$ is that it is independent of molecular weight. An important interpretation of $\zeta$, originally given by Edwards[39] and later amplified by Daoud[41,42] and de Gennes,[40] is that it is also related to an intramolecular correlation length. At size scales less than $\zeta$ a chain only interacts with itself and correlations among monomers must be of the self-excluded-volume type. At size scales larger than $\zeta$, the chain interacts with other chains and the self-excluded-volume interactions are screened. Of course, through a polymer/polymer interface, the $\zeta$ for each polymer continuously changes. In a mean-field theory,[39,40] $\zeta \sim c^{-1/2}$ and thus one might argue that the coefficient of the corresponding square gradient term should vary as $c^{-1}$. This is the result obtained in HS theory[14] (see their eq 3.2).

## References and Notes


(1) Poser, C. I.; Sanchez, I. C. *J. Colloid Interface Sci.* **1979**, *69*, 539.
(2) Sanchez, I. C.; Lacombe, R. H. *J. Phys. Chem.* **1976**, *80*, 2352.
(3) Lacombe, R. H.; Sanchez, I. C. *J. Phys. Chem.* **1976**, *80*, 2568.
(4) Sanchez, I. C.; Lacombe, R. H. *J. Polym. Sci., Polym. Lett. Ed.* **1977**, *15*, 71.
(5) Sanchez, I. C.; Lacombe, R. H. *Macromolecules* **1978**, *11*, 1145.
(6) van der Waals, J. D. *J. Phys. Chem.* **1894**, *13*, 657.
(7) Cahn, J. W.; Hilliard, J. E. *J. Chem. Phys.* **1958**, *28*, 258.
(8) Cahn, J. W. *J. Chem. Phys.* **1959**, *30*, 1121.
(9) Bongiorno, V.; Scriven, L. E.; Davis, H. T. *J. Colloid Interface Sci.* **1976**, *57*, 462.
(10) Carey, B. S. Ph.D. Thesis, University of Minnesota, 1979.
(11) Gaines, G. L., Jr. *J. Polym. Sci., Part A-2* **1971**, *9*, 1333.
(12) Nose, T. *Polym. J.* **1976**, *8*, 96.
(13) Vrij, A.; Roeberson, G. T. *J. Polym. Sci., Polym. Phys. Ed.* **1977**, *15*, 109.
(14) Helfand, E.; Sapse, A. M. *J. Chem. Phys.* **1975**, *62*, 1327.
(15) Helfand, E.; Tagami, Y. *J. Chem. Phys.* **1972**, *56*, 3592.
(16) Roe, R. J. *J. Chem. Phys.* **1975**, *62*, 490.
(17) Wu, S. *Polym. Blends. 1978* **1978**, *1*, 244–95.

(18) Kammer, H. W. *Faserforsch. Textiltech.* **1978**, *29*, 459.
(19) Joanny, J. F.; Leibler, L. *J. Phys. (Paris)* **1978**, *39*, 951.
(20) van der Waals, J. D.; Kohnstamm, Ph. "Lehrbuch der Thermodynamik"; Maas and van Suchtelen: Leipzig, 1908; Vol. I, p 207.
(21) Sanchez, I. C. *J. Macromol. Sci., Phys.* **1980**, *B17*, 565.
(22) Carey, B. S.; Scriven, L. E.; Davis, H. T. *AICHE J.* **1980**, *26*, 705.
(23) Poser, C. I. Ph.D. Thesis, University of Massachusetts, 1980.
(24) Diaz Pena, M.; Menduina, C. *J. Chem. Thermodyn.* **1974**, *6*, 1097.
(25) Diaz Pena, M.; Delgado, J. N. *J. Chem. Thermodyn.* **1975**, *7*, 201.
(26) Harsted, B. S.; Thomson, E. S. *J. Chem. Thermodyn.* **1974**, *6*, 549.
(27) Letcher, T. M. *J. Chem. Thermodyn.* **1975**, *7*, 205.
(28) Hsu, K. Y.; Clever, H. L. *J. Chem. Thermodyn.* **1975**, *7*, 435.
(29) Ridgway, K.; Butler, P. A. *J. Chem. Eng. Data* **1967**, *12*, 509.
(30) Schmidt, R. L.; Clever, H. L. *J. Colloid Interface Sci.* **1968**, *26*, 19.
(31) Schmidt, R. L.; Randall, J. C.; Clever, H. L. *J. Phys. Chem.* **1966**, *70*, 3912.
(32) Prigogine, I.; Marechal, J. *J. Colloid Interface Sci.* **1952**, *7*, 122.
(33) Gaines, G. L., Jr. *J. Phys. Chem.* **1969**, *73*, 3143.
(34) Siow, K. S.; Patterson, D. *J. Phys. Chem.* **1973**, *77*, 356.
(35) Leimmermans, J. "Physical-Chemical Constants of Binary Systems in Concentrated Solutions"; Interscience: New York, 1959; Vol. I.
(36) Widom, B. In *Phase Transitions Crit. Phenom.* **1972**, *2*.
(37) Yang, A. J. M.; Fleming, P. D., III; Gibbs, J. H. *J. Chem. Phys.* **1976**, *64*, 3732. *Ibid.* **1976**, *65*, 7.
(38) Edwards, S. F. *Proc. Phys. Soc., London* **1965**, *85*, 613.
(39) Edwards, S. F. *Proc. Phys. Soc., London* **1966**, *88*, 265.
(40) de Gennes, P. G. "Scaling Concepts in Polymer Physics"; Cornell University Press: Ithaca, NY, 1979; Chapter 3.
(41) Daoud, M., et al. *Macromolecules* **1975**, *8*, 804.
(42) Daoud, M. *J. Polym. Sci., Polym. Symp.* **1977**, *61*, 305.
(43) Egelstaff, P. A.; Widom, B. *J. Chem. Phys.* **1970**, *53*, 2667.
(44) Bhatia, A. B.; March, N. H. *J. Chem. Phys.* **1978**, *68*, 1999.
(45) Henderson, J. R. *Mol. Phys.* **1980**, *39*, 709.

# Critical Exponents in Polymers: A Sol–Gel Study of Anionically Prepared Styrene–Divinylbenzene Copolymers

**Manfred Schmidt and Walther Burchard***

*Institute of Macromolecular Chemistry, University of Freiburg, D-7800 Freiburg, West Germany.* *Received July 18, 1980*

ABSTRACT: Anionic copolymerization of divinylbenzene (DVB) with styrene (St) leads at low ratios of $R$ ([DVB]/[initiator]) to branched polymers which beyond $R_c = 15.1$ form macroscopic gels. A sol–gel separation has been carried out. Molecular weights $M_w$ and $M_n$ and radii of gyration $\langle S^2 \rangle_z^{1/2}$ of samples from the pregel and postgel have been measured by light scattering and plotted as functions of $\epsilon = |1 - (1 - r)R/(1 - r_c)R_c|$, where $r$, which could be determined from measurement of $M_n$, is the extent of ring formation of the second double bonds from the DVB units. The critical exponents so far determinable by experiment tend to support the Flory–Stockmayer (FS) theory rather than percolation theory. Because of the large extent of ring formation, full agreement is not obtained with the classical FS theory, as expected, since this theory neglects the long-range correlation effects associated with ring formation.

## Introduction

Critical phenomena have been known since 1869 when Andrews[1] reported a phase diagram of carbon dioxide. Since then, a large number of critical systems have been discovered in physics and in physical chemistry, and much effort has been invested in a theoretical description of these phenomena. Mainly two controversial concepts have been developed. First and powerful success was achieved by theories which are now called mean-field theories (e.g., the van der Waals equation for the gas–liquid phase transition,[2] Weiss treatment of ferromagnetism,[3] and Flory–Huggins theory for liquid–liquid phase transitions mainly in polymers[4,5]). With Ising's famous treatment of one-dimensional ferromagnetism[6] by a first-order Markovian process, it has become more and more common to take into consideration nearest-neighbor interactions and the resulting cooperative nature of the critical phenomena. Extension of Ising's calculation to three-dimensional lattices has challenged many scientists, but so far an exact solution has only been found for the two-dimensional case by Onsager.[7] Computer simulations and approximate theories,[8-11] for instance, the scaling theory[12] and, more recently, the renormalization group theory,[13,14] have revealed, however, some relationships between the so-called critical exponents. According to these developments the properties of a system depend, in the vicinity of the critical point, on a function $\epsilon = (1 - T/T_c)$ with exponents which substantially deviate from the mean-field exponents ($T$ and $T_c$ are the temperatures at a given and at the critical point). A large number of measurements give strong evidence for these non-mean-field exponents.[9-11,15]

The astounding similarity of these exponents in quite different critical systems has led theoreticians to the hypothesis of universality for all critical phenomena. With this background, the recent interest of theoretical physicists in gelation processes becomes understandable, because this process is now considered unanimously as a critical phenomenon. It is useful, however, to stress the difference of this gelation phenomenon from the critical phenomena mentioned above.

(i) Most gelation processes in polymer science are, in practice, irreversible; i.e., once formed, the gel cannot simply be transformed into a solution by changing the temperature within a short interval of $\epsilon$.

(ii) Gelation is not influenced by thermodynamic interaction of nearest-neighbor monomeric units. Instead, the process is controlled by kinetic equations and the resulting probabilities or extents of reaction, $\alpha$.

(iii) The behavior of measurable quantities is determined by a reduced parameter $1 - \alpha/\alpha_c$ which takes the role of $\epsilon$ in the thermodynamic reversible critical phenomena.

Between 1941 and 1945 a theory of branching and gelation of polymers was developed by Flory and by Stockmayer.[16-20] This classical theory (hereafter FS) gives for the $f$-functional *random* polycondensation a very satisfactory prediction of the gel point and of the increase in

0024-9297/81/2214-0370$01.25/0 